Skupljanje morta s dodatkom pepela drvne biomase i recikliranih polimernih vlakana iz otpadnih guma

Grubor, Martina; Carević, Ivana; Serdar, Marijana; Štirmer, Nina

Source / Izvornik: **Građevinar, 2023, 75, 367 - 378**

Journal article, Published version
Rad u časopisu, Objavljena verzija rada (izdavačev PDF)

https://doi.org/10.14256/JCE.3642.2022

Permanent link / Trajna poveznica: https://urn.nsk.hr/urn:nbn:hr:237:854977

Primljen / Received: 10.11.2022.
Ispravljen / Corrected: 9.3.2023.
Prihvaćen / Accepted: 16.3.2023.
Dostupno online / Available online: 10.5.2023.

Shrinkage of mortar with the addition of wood biomass ash and recycled tyre polymer fibres

Authors:

Martina Grubor, PhD. CE
University of Zagreb
Faculty of Civil Engineering
martina.grubor@grad.unizg.hr

Ivana Carević, PhD. CE
University of Zagreb
Faculty of Civil Engineering
ivana.carevic@grad.unizg.hr

Assoc.Prof. **Marijana Serdar**, PhD. CE
University of Zagreb
Faculty of Civil Engineering
marijana.serdar@grad.unizg.hr

Prof. **Nina Štirmer**, PhD. CE
University of Zagreb
Faculty of Civil Engineering
nina.stirmer@grad.unizg.hr
Corresponding author

Original research paper

Martina Grubor, Ivana Carević, Marijana Serdar, Nina Štirmer

Shrinkage of mortar with the addition of wood biomass ash and recycled tyre polymer fibres

In this paper, the possible synergistic effects of fly wood biomass ash (WBA) and recycled tire polymer fibres (RTPF) on long-term autogenous shrinkage and drying shrinkage in mortar were investigated, and the pore structures of mortar specimens with WBA and RTPF were determined. The results showed that the use of RTPF and WBA has an effect on the pore structure of mortars and thus on the results of autogenous shrinkage. When WBA and RTPF were used, the autogenous shrinkage tended to decrease; however, this was not the case for the drying shrinkage. The greatest reduction in autogenous shrinkage was achieved by the addition of WBA and RTPF; autogenous shrinkage was reduced by 62 % after 90 days compared with the reference mixture.

Key words:
wood biomass ash, recycled tyre polymer fibres, drying shrinkage, autogenous shrinkage, pore size distribution

Izvorni znanstveni rad

Martina Grubor, Ivana Carević, Marijana Serdar, Nina Štirmer

Skupljanje morta s dodatkom pepela drvne biomase i recikliranih polimernih vlakana iz otpadnih guma

U ovom istraživanju istražen je mogući sinergijski učinak upotrebe pepela drvne biomase (PDB) i recikliranih polimernih vlaka iz otpadnih guma (RTPF) na dugotrajno autogeno skupljanje i skupljanje uslijed sušenja, te je određena struktura pora uzorka morta s dodatkom PDB-a i RTPF-a. Rezultati pokazuju da primjena PDB-a i RTPF-a u mortovima utječe na strukturu pora, a time i na rezultate autogenog skupljanja. Kada se koriste PDB i RTPF, autogeno se skupljanje smanjuje, što nije slučaj za skupljanje uslijed sušenja. Najveće smanjenje autogenog skupljanja postignuto je dodatkom PDB-a i RTPF-a: autogeno skupljanje smanjeno je za 62 % nakon 90 dana u usporedbi s referentnom mješavinom.

Ključne riječi:
pepeo drvne biomase, reciklirana polimerna vlakna iz otpadnih guma, skupljanje uslijed sušenja, autogeno skupljanje, raspodjela veličine pora

1. Introduction

In cement composites, owing to exposure to a certain temperature and humidity, shrinkage frequently occurs owing to drying caused by the withdrawal of water from the porous structure of concrete by evaporation and diffusion [1]. The lack of water for hydration causes the cement composition to dry, leading to autogenous shrinkage. In other words, autogenous deformation is the total macroscopic volume change in a closed isothermal cement composite system [2, 3]. Volume deformation caused by the shrinkage of cement composites is one of the main causes of crack formation. Cracks in cement composites can increase in size during use, increasing the risk of penetration of aggressive substances from the environment into the microstructure of the composite. Volume deformation depends on the composition of cement composites, the temperature and humidity of the environment, and the dimensions of the structural element [1, 2]. In addition, adjustments in the concrete composition and the use of various chemical and mineral admixtures and fibres can reduce the shrinkage of cement composites, including both autogenous shrinkage and drying shrinkage [1, 4-7].

Numerous studies on concrete have shown that many industrial waste products improve certain properties of concrete depending on the purpose for which they are developed, making them extremely valuable raw materials whose use reduces harmful effects on the environment. Waste materials with significant potential for use in concrete include wood biomass ash (incineration ash produced when wood biomass is burned in an industrial process) and recycled tire polymer fibres (by-products of recycling waste tyres).

Wood biomass ash (WBA), produced by biomass incineration, is a complex mixture of inorganic and organic materials, the volume, properties, and quality of which vary more than those of conventional coal fly ash, depending on various parameters [8]. Moreover, WBA consists of very small particles that can be easily transmitted through the air, which can cause health problems related to the respiratory system in populations living near WBA landfills [9]. Moreover, if the temporary disposal of WBA is inadequate, it can cause groundwater pollution [10]. However, research has shown that WBA can be reused in the concrete industry as a substitute for cement or aggregates owing to its properties and chemical composition [10-12]. The partial replacement of cement with WBA reduces drying shrinkage [13-15]. Previous studies have concluded that lower drying shrinkage values can be explained by the fact that WBA acts as a filler rather than a binder. In a study by [16], 20 % WBA from the bottom of a furnace reduced drying shrinkage by up to 11.9 % compared with the reference mortar mixture, and lower hydration temperatures led to lower shrinkage values and a later pozzolanic reaction of the material used. In contrast, reference [17] indicated that 17.5 % fly WBA as cement replacement had no effect on shrinkage, whereas higher proportions of WBA resulted in higher drying shrinkage compared with the reference mixture. This is because the dimensional changes are primarily caused by the porosity of the material, and additional pre-treatment with WBA (particularly additional burning and removal of light particles) can positively influence drying shrinkage. The characterisation of WBA (high free CaO and MgO content) and volume stability ('soundness') testing in reference [18] suggested that the expansion potential of WBA can be used advantageously to mitigate autogenous shrinkage problems by using it as an expansive additive owing to its high free CaO and MgO content.

Recycled tire polymer fibres (RTPF), by-products of recycling waste tyres, are high-value materials used as a fuel in cement production. However, most RTPF are still disposed of exclusively in landfills. Owing to its low volumetric mass, ease of transport by wind, and high flammability, approximately 250,000 t of this waste material is generated annually in the EU [19]. Recent studies on RTPF have shown that the addition of this type of fibre to a fresh concrete mixture does not affect the workability properties of the concrete, while ensuring the reduction of early age deformations and restrained shrinkage with an insignificant effect on the compressive strength [19-24]. In addition, RTPF prevent explosive spalling in heated concrete with insignificant effects on the mechanical properties and durability of concrete [25-27] and improves the behaviour of concrete when exposed to aggressive environments [19, 21] and the mechanical behaviour under high strain rate and cyclic loading [28, 29].

In this study, the shrinkage behaviour and pore structure of mortars containing fly wood biomass ash and recycled tire polymer fibres were investigated. The main objectives of this study were to:

- determine the synergistic effect and influence of fly WBA and RTPF on the long-term autogenous and drying shrinkage of mortar
- determine the pore structure of mortar samples with fly WBA and RTPF. In addition, the mechanical properties of the fresh composites were investigated.

2. Materials and methods

2.1. Materials

In this study, the cement used was CEM I 42.5 R, which consists of 95 % to 100 % Portland clinker and 0 %–5 % by-products. It is characterised by a very high early strength, rapid setting time, and the development of a high heat of hydration. In addition, standardised quartz sand and potable water were used to produce the mortars. The water was stored in plastic containers under laboratory conditions to ensure a constant temperature of 20 ± 2 °C. In addition, recycled polymer fibres from waste tyres, which are frequently heavily contaminated with residual rubber during the mechanical recycling of waste tyres, were used. Therefore, the RTPF were further cleaned using an innovative device for cleaning fibres [19]. The properties of the cleaned RTPF are listed in Table 1.

In this study, the fly WBA used was collected from a power plant using grate combustion technology. WBA is obtained by

Table 1. Properties of RTPF [20]

Length [mm]	**Diameter** [μm]		**Density** [g/cm³]	**Chemical composition**
9.5 ± 4.6	type 1	30.1 ± 2.0	1.32	Approximately 60 % (poly ethylene-terephthalate - PET), 25 % PA 66 (polyamide 66) and 15 % (poly butylene terephthalate - PBT)
	type 2	20.2 ± 1.7		
	type 3	12.4 ± 1.8		

Table 2. Mortar mixtures

Mixture name	**Mixture description/dosage**	
	Fly wood biomass ash	**Recycled tyre polymer fibres**
M1	--	-
M2	-	2 kg/m³
M3	15 % WBA as cement replacement	-
M4	15 % WBA as cement replacement	2 kg/m³

burning beech, oak, fir, and spruce at an average temperature of 700–950 °C. During wood biomass combustion, the power plant uses clean wood chips with impurities (soil and stones) and residues from wood extraction, green wood chips (wood chips made from fresh roundwood and residues from thinning, including branches and tops).

2.2. Methods for WBA characterization

Thermogravimetric (TG) measurements of the WBA samples were performed on a LECO TGA 701 instrument using a ceramic vessel filled with approximately 1 g of the powder sample. The temperature interval of the measurement ranged from 35 to 950 °C at a heating rate of 20 °C/min, using inert gas (nitrogen, flow: 30 mL/min) to prevent oxidation during the measurement. Before measurement, samples were dried at 35 °C for 15 min to remove moisture.

The particle size distribution was examined using laser diffraction using a SALD 3101 instrument (Shimadzu), with the samples dispersed in an air stream at a pressure of 0.4 MPa. Fraunhofer theory was applied to calculate the particle size based on the diffraction angle.

The morphology of the WBA samples was observed via scanning electron microscopy (SEM) using an SEM FE MIRA II LMU instrument. Before imaging, the samples were sputtered with a gold/palladium (Au/Pd) layer in argon (Ar) plasma.

The chemical compositions of the WBAs were tested according to the procedure prescribed in EN ISO 16948:2015. Their pH values were determined according to EN 12176:2005, and the loss of ignition (LOI) was evaluated according to EN 15168:2009. The density of the WBA was tested using the Le Chatelier flask method according to ASTM C-188.

2.3. Mixture design and testing methods

The specimens were fabricated with CEM I 42.5 R cement, potable water, and standard sand according to EN 196-1 [30]. The composition of the mortar was determined according to the standard EN 196-1:2016 [30], with a mass ratio of CEN sand, cement, and water of 3:1:0.5, and a water-binder ratio of 0.5. Table 2 lists the different mixtures that were tested, including a description of each mixture.

Cement mortar samples were prepared according to the procedure given by [30]. The prepared mortars were poured into steel moulds with dimensions 40 × 40 ×160 mm. The fresh state properties of the mortars were determined immediately after mixing. After demoulding, the specimens were stored in a humid room at 20 ± 2 °C and RH ≥ 95 %, until the compressive and flexural strength tests. A different curing procedure was used for the drying shrinkage test. Table 3 shows the test standards used to evaluate the mortar properties prescribed in the experimental program and the number of specimens for each property per mixture or age. All methods used to test fresh and hardened concrete properties were standardised, except for the methods used for long-term volume deformations and pore size distribution.

Table 3. Tests methods

Test method	**Standard**	**Number of specimens (per mixure/age)**
Density	HRN EN 1015-6:2000/A1:2008	-
Temperature	U.M1.032:1981	-
Pore content	HRN EN 1015-7:2000	-
Consistence by flow table	HRN EN 1015-3:2000/A1:2005/A2:2008	-
Compressive strength and flexural strength	HRN EN 196-1:2016	3
Drying shrinkage	HRN EN 12617-4:2003	3
Autogenous shrinkage	-	3
Pore size distribution	Mercury intrusion porosimeter	1

2.3.1. Drying shrinkage

Manual measurements of the drying shrinkage were performed on three prismatic specimens with dimensions of 40 × 40 × 160 mm^3. The specimens were stored at 21 ± 2 °C and RH 60 ± 10 %. Measurements were performed at 1, 3, 7, 14, 28, 42, 56, 90, and 365 days of age using a Graff-Kaufmann instrument, with an accuracy of 1 μm.

2.3.2. Autogenous shrinkage

The autogenous deformation test was performed on prisms with dimensions of 40 × 40 × 160 mm^3 according to [31]. Before the mortar was poured, the moulds were coated with a polyethylene film (the area connecting the side films was sealed with silicone, and the sealing areas of the measuring rappers and side edges of the coated film were preferably sealed with silicone). After casting, the specimens were taped to completely prevent drying and evaporation of moisture (Figure 1.a).
The mortar was first poured into the mould to half the height of the mould, and the specimen was shaken on a shaking table, after which the mortar was poured up to the top of the mould and shaken again. The specimens were sealed to eliminate moisture loss. They were covered with plastic film and sealed with two layers of tape. After 24 h, the specimens were demoulded and immediately wrapped in two layers of aluminium foil, which has been shown to be very effective in preventing moisture loss [31]. The prepared specimens are shown in Figure 1.b and 1.c. When the samples were wrapped in aluminium foil, an initial measurement of the length and mass change was performed. The samples were then placed in a plastic bag and stored in a humid chamber at a temperature of 20 ± 2 °C and a relative humidity (RH) of 95 %. The length and mass changes were measured after 1, 3, 7, 14, 28, 56, and 90 days. The measurement performance is shown in Figure 1.c. Three samples were prepared from each mixture.

2.3.3. Mercury intrusion porosimeter on mortar specimens

Measurements were performed using a Micromeritics AutoPore IV 9500 porosimeter, considering the Washburn equation and assuming a contact angle of 130° and a surface tension of 0.485 N/m. All the MIP measurements were performed within a pressure range of up to 414 MPa with an equilibrium interval of 10 s.
Before the measurement, the samples were cut into smaller pieces. To stop the hydration, free water was removed by immersing the crushed sample in isopropanol for 24 h. Excess isopropanol was removed via vacuum filtration and washed with diethyl ether to shorten the solvent evaporation time. Before analysis, samples were oven dried at 60 °C for two days. One sample was obtained from each mixture and curing condition (RH of 60 ± 10 % and temperature of 21 ± 2 °C for drying shrinkage and RH of 95 % and temperature of 20 ± 2 °C for autogenous shrinkage). The MIP results of the specimens for drying shrinkage were marked as Mi-S, whereas those for autogenous shrinkage were marked as Mi-A.

Figure 1. Testing of autogenous deformation: a) prepared mould; b) samples coated with aluminium foil; c) measuring rappers

3. Results and discussion

3.1. Material characterisation

The chemical and physical properties of the WBA and cement are listed in Table 4. Based on the chemical and physical properties of WBA and the criteria of the standard EN 450-1 [32], a higher proportion of alkalis was observed, particularly a higher proportion of potassium oxide, which is an integral component of wood biomass [33]. The percentage of MgO was 6.17 %, exceeding the limits criteria specified by the standard (<4 wt. %). Free CaO was not measured, but higher values can be expected depending on the aging of the WBA [34]. Higher amounts of free CaO and MgO must be avoided, as this can lead to expansion, cracking, and strength loss of the hydrated material [18]. Compared with coal fly ash [32], WBA has a higher proportion of CaO and lower proportion of pozzolanic oxides (SiO_2, Al_2O_3, and Fe_2O_3), indicating lower pozzolanic activity and pronounced hydraulic activity [35, 36]. The limits for sulphates (≤ 3 wt. %), phosphates (≤ 5 wt. %), and loss on ignition (LOI) for class A (≤ 5 wt. %) provided in EN 450-1 are satisfied by WBA as a mineral admixture in cement composites. The cement particles had a finer distribution than in the WBA sample (Figure 2.b).
In this study, aged WBA was used for the mixtures, which was stored in closed plastic bags for six months from the day of collection from the power plant. The shelf life and changes in the properties of WBA in a closed environment were investigated in detail in [37]. Because of the high content of free CaO in the WBA samples, a carbonation process was expected, which means that free CaO can spontaneously hydrate and carbonate under humid conditions, thus reducing the free CaO [38, 39]. This process is beneficial for the application of WBA, as

the proportion of free CaO can affect the volume stability and durability when used in cement composites [18, 40].

Table 4. Chemical and physical properties of WBA and cement

Component	CEM I 42.5 R	Wood biomass ash (WBA)	Criteria according to HRN EN 450-1. % mass.
P_2O_5	0.217	1.97	≤ 5
Na_2O	0.846	0.57	/
K_2O	1.25	8.10	/
CaO	59.8	57.93	/
MgO	2.01	6.17	< 4
Al_2O_3	4.94	3.14	/
TiO_2	0.231	0.13	/
Fe_2O_3	3.15	2.1	/
SiO_2	21.88	18.19	/
Pozzolanic oxides	29.97	23.43	≥ 70
Na_2O_{eq}	1.67	5.90	≤ 5
SO_3	3.33	1.7	≤ 3
LOI (950 °C)	3.6	3.0	≤ 5 for A class
pH	-	13.15	/
d_{50}, µm	1.0	18.6	/

Author [38] examined the influence of fresh and aged WBA on the volume stability of cement properties when WBA was used as a cement replacement. WBA obtained directly from power plants and used immediately as 10 % and 15 % cement replacements in cement mixtures did not satisfy the requirements of the standard EN 450-1 standard because it contained a high percentage of free CaO (39.96 wt. %). However, after WBA stabilisation, all the tested cement composites satisfied the volume stability test criteria, with the maximum free CaO content in the stabilised WBA samples being 20.49 mass %. TG measurements were performed to determine the phase transformations of the collected (fresh) and aged (when used) WBA (Figure 2a). Two phases were expressed: weight loss of approximately 400 °C and weight loss greater than 600 °C. A significant decrease in mass loss greater than 600 °C is attributed to a large proportion of $CaCO_3$, whereas a mass loss in the range of 400–500 °C is attributed to decomposition of portlandite, $Ca(OH)_2$ to CaO and H_2O [41]. In the aged WBA, a higher portlandite content was visible, suggesting that free lime is stabilised over time [37].

The SEM analysis of the WBA samples revealed mostly irregular structures, inhomogeneous particle surfaces, and differently shaped particles compared with coal fly ash (Figure 3). This observation was consistent with previous studies [12, 42].

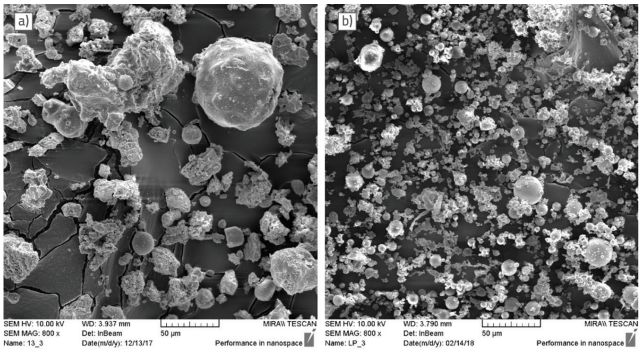

Figure 3. Micrographs of WBA and coal fly ash (magnification SEM_MAG = 800×)

3.2. Fresh state properties

The test results for the fresh properties (pore content, density, temperature, and consistency) are shown in Table 5, and the influence of WBA and RTPF on consistency (by flow table) is shown in Figure 4.

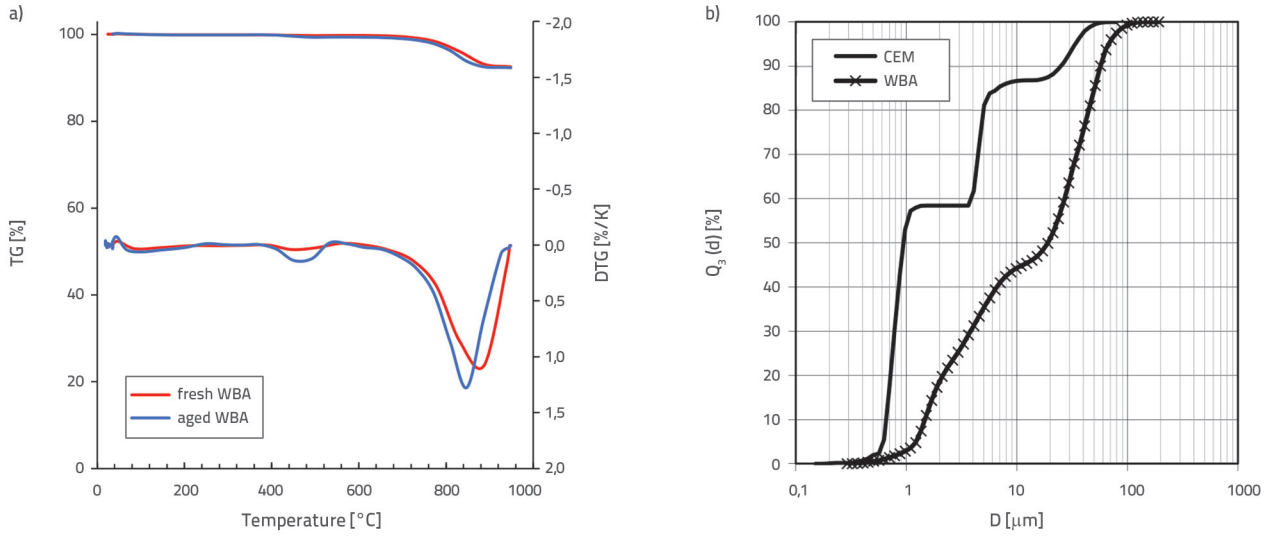

Figure 2. a) TG measurement of the fresh and aged WBA sample; b) laser diffraction of the materials used

Table 5. Results of the fresh properties of the mortars

Properties \ Mixture	M1	M2	M3	M4
Density [kg/m³]	2205	2183	2174	2167
Temperature [°C]	22.3	22.3	22.0	21.5
Pore content [%]	5.9	6.5	6.0	6.0
Consistency [mm]	195	170	165	150

The consistency of all test mixtures ranged from 150 to 195 mm. The results showed that the replacement of cement with WBA and the addition of RTPF led to a decrease in workability. The replacement of cement with WBA resulted in an 18 % decrease in workability compared with the reference mixture M1, whereas the addition of 2 kg/m³ RTPF decreased workability by 15 %. A significant decrease in workability was observed in mixture M4 (with WBA and RTPF), where the loss of workability was 30 % compared with M1. The temperatures of the mortar mixes ranged from 21.5 °C (for M4) to 22.3 °C (for M1 and M2).

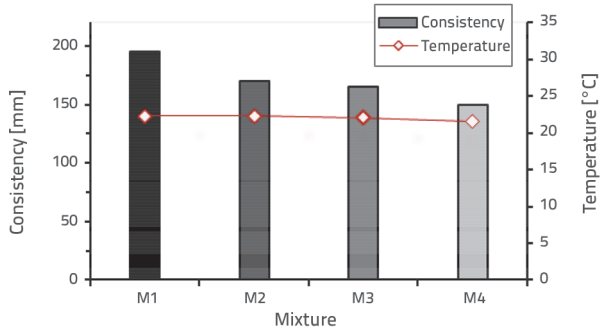

Figure 4. Results of testing consistency and temperature

The density of the studied mixtures ranged from 2.17 kg/dm³ (for M4) to 2.21 kg/dm³ (for the reference mixture without WBA and RTPF). The differences in density between the mixtures were up to 2 %, which showed that WBA and RTPF did not significantly affect the mortar density. The results of the air content test showed that the mixture with 2 kg/m³ RTPF had a higher value (6.5 %) compared with M1 (5.9 %). Thus, the addition of RTPF led to an increased pore content of 10 % in the fresh mortar. The replacement of cement with 15 % WBA had a minor effect on the air content (up to 1 %). M4 with a combination of RTPF and WBA also had a small effect on the air content (up to 1 %) compared with the reference mixture. The combination of WBA and RTPF minimised the degradation effect of the fibres on the air content.

The analysis of the mortar properties in the fresh state revealed the influence of WBA and RTPF addition on the consistency of the cement composites, i.e. a decrease in consistency from 15 % (M2) to 30 % (M4) compared with the reference. This was consistent with previous studies on the use of WBA in cement composites [17, 18, 34, 43-45]. Irregularly shaped and porous WBA particles tend to absorb water, which can negatively affect the workability of the composites [34, 46, 47]. The statistical analysis in [34] showed the influence of alkali content on water demand: the higher the alkali content, the higher the water requirement. The WBA used in this study had a higher alkali content than cement (5.90 % vs. 1.67 %).

3.3. Mechanical properties

The results of the compressive strength tests conducted at 28 days of age, together with their absolute deviations, are shown in Figure 5.a. The compressive strengths of the tested mixtures ranged from 50.2 MPa (for M4) to 74.1 MPa (for M2). Compared with the reference mixture without fibres and WBA, the addition of RTPF in an amount of 2 kg/m³ resulted in a small difference in compressive strength (increase of less than 8 %), whereas the replacement of 15 % of the cement with WBA decreased the compressive strength by 19 %. The compressive strength of M4 with 15 % WBA content and 2 kg/m³ RTPF decreased by 30 % (50.2 MPa) compared with the reference mixture.

The results of the flexural strength tests conducted at 28 days of age and their absolute deviations are shown in Figure 5.b. The flexural strength values of the tested mixtures ranged from 7.25 MPa (for M3) to 8.17 MPa (for M2). Compared with the reference mixture without fibres and WBA, the addition of RTPF did not significantly affect the flexural strength (increase of only 1 %), whereas the replacement of 15 % of the cement with WBA decreased the compressive strength by 11 %. The flexural

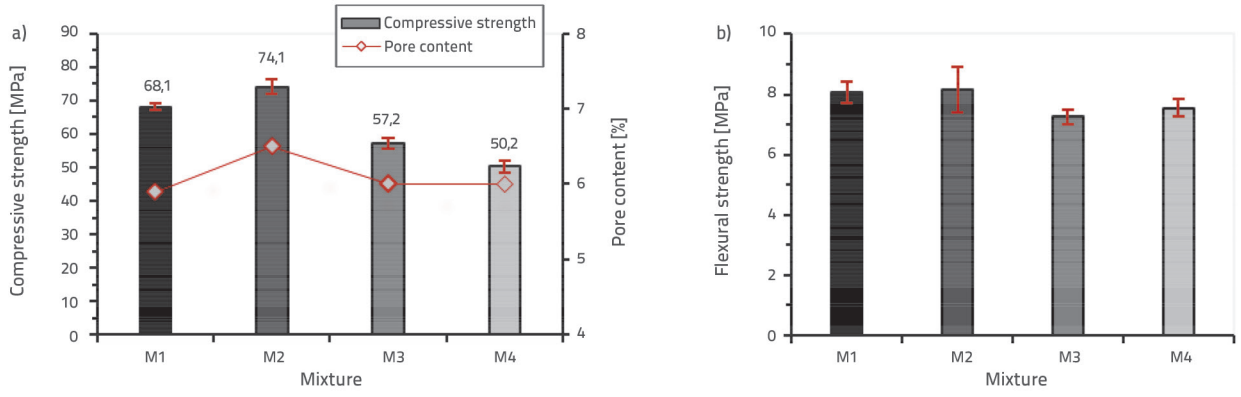

Figure 5. Average results of strength tests at 28 days of age: a) compressive strength; b) flexural strength

strength of M4 with 15 % WBA content and 2 kg/m³ RTPF decreased by 8 % compared with the reference mixture. For these mixtures, we observed that the replacement of cement by 15 % WBA reduced the flexural strength by approximately 10 % at 28 days of age.

The results of the mechanical properties (compressive and flexural strengths) indicate that the replacing cement with 15 % WBA reduced the values after 28 days. The same trend was observed for the mixtures in which RTPF and WBA were used. However, we can generally conclude that mortars with a WBA of 15 % have a compressive strength above 50 MPa, which is acceptable for use in practice.

3.4. Dimensional stability

The drying shrinkage may reflect the dimensional stability of cementitious materials in a drying environment. Figure 6 shows the effects of WBA and RTPF on drying shrinkage for up to 365 days.

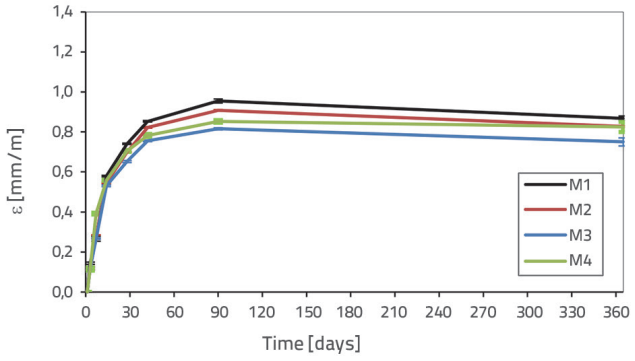

Figure 6. Drying shrinkage of mortars of different ages up to 365 days

The total drying shrinkage after 90 days in order of decreasing values for the tested mixtures (Figure 6) was as follows: M1 (0.95553 mm/m ± 0.0098) > M2 (0.908 mm/m ± 0.0039) > M4 (0.883 mm/m ± 0.0063) > M3 (0.816 mm/m ± 0.0053). Furthermore, the total drying shrinkage after 365 days in order of decreasing values for the tested mixtures was as follows: M1 (0.8683 mm/m ± 0.0117) > M2 (0.8273 mm/m ± 0.0042) > M4 (0.8250 mm/m ± 0.0248) > M3 (0.7504 mm/m ± 0.0198).

The results presented in Table 6 indicate that the partial substitution of cement with WBA and the use of RTPF contributed to an average reduction in overall deformations of 5 % (M2), 17 % (M3), and 12 % (M4) compared with the control mortar after 90 days. After 365 days, a difference in the behaviour of M4 was observed. The contribution to the reduction in the overall deformation was smaller that of the control mixture at 90 days; the reduction was 5 %, whereas the other mixtures exhibited a similar behaviour to that at 90 days. The largest contribution to the reduction in drying shrinkage at 365 days of age s observed in specimens with 15 % WBA as cement replacement, i.e. the reduction in shrinkage was 14 %, which was almost equal to the percentage of cement replacement by WBA. The same trend was observed in [19], whose trend of decreasing drying shrinkage was correlated with the proportion of free CaO: the higher the proportion of free CaO, the greater the expected decrease in drying shrinkage. When 2 kg/m³ of RTPF were added, a 5 % reduction in drying shrinkage was observed compared with the control mixture. In a previous study, Chen et al. [48] observed that increasing the RTPF dosage in mortar mixtures consistently resulted in improved shrinkage performance, with the largest improvement being 22.43 % (for a mixture containing 2 % RTPF by volume) compared with a mixture without RTPF. Serdar et al. [22] observed a different trend; the addition of RTPF at different dosages had a minor or no effect on the drying shrinkage of concrete. The reduction in drying shrinkage of the M3 samples, where 15 % WBA was used, corresponded to a reduction in cement content in the specimens. Additionally, in the mixtures in which RTPF and WBA were used individually (M2 and M3), shrinkage was reduced. However, no synergistic effect was observed when used together in M4; the difference between the control mixtures and M4 was the same as that when only fibres were used. Therefore, we can conclude that the addition of WBA had no effect on the drying shrinkage.

Table 6. Changes in drying shrinkage compared with the reference mixture

Age	M2	M3	M4
90 days	-4.9 %	-14.6 %	-10.7 %
365 days	-4.7 %	-13.6 %	-5.0 %

The results of the long-term autogenous shrinkage are shown in Figure 7, and the relative decreases (positive values) or increases (negative values) for specimens M2, M3, and M4 compared with the reference mixtures are listed in Table 7.

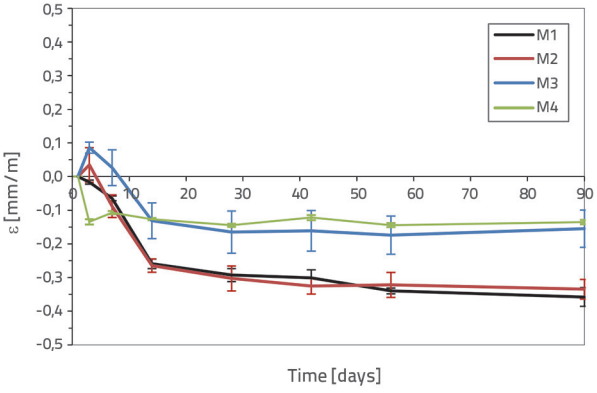

Figure 7. Autogenous shrinkage of mortars at different ages up to 90 days

In this case, in terms of the autogenous shrinkage, the highest values were obtained for M1, whereas the lowest values were obtained for M4 with 15 % WBA and 2 kg/m³ RTPF. The results of the autogenous shrinkage test after 90 days were (absolute value, from higher to lower) M1 (0.3577 mm/m ± 0.0276) > M2 (0.3346 mm/m ± 0.0291 > M3 (0.1549 mm/m ± 0.0554 > M4 (0.1353 mm/m ± 0.0123). The results of the autogenous

shrinkage test after 90 days for M2, M3, and M4 were 6.4 %, 56.7 %, and 62.2 % lower than reference mixtures, respectively (Table 7). This was particularly pronounced in M3 and M4, where autogenous shrinkage was significantly lower, more than 15 % of cement was replaced with WBA. When comparing the individual values of autogenous shrinkage for mixtures with WBA and RTPF (M2 and M3), swelling occurred up to the age of 7 days (Figure 7 and Table 7) and disappeared with increasing hydration time. One possible solution for controlling cracking owing to autogenous shrinkage is to use materials that exhibit initial expansion. The most common method for producing expansive cement is the formation of ettringite, where expansion occurs through the growth of preferentially oriented ettringite crystals. Other possibilities include hydration of free lime (CaO) or periclase (MgO) [49]. A detailed characterisation of the WBA revealed high levels of free Mg and CaO [13, 18], which could be used to reduce autogenous shrinkage. According to previous studies, the reduction in autogenous shrinkage is influenced by the production of the CH phase [50] and the formation of ettringite [51] at early ages. The increased autogenous shrinkage values at early ages for mixtures with WBA can be explained by the formation of portlandite. The maximum Ca $(OH)_2$ content during WBA hydration was reached after 3 days [18], which correlated with the swelling in the autogenous shrinkage results. As the hydration progressed, the proportion of portlandite decreased, indicating a pozzolanic reaction. When studying the pozzolanic reaction of WBA samples, reference [36] demonstrated that WBA alone reacts with water-consuming free lime to form portlandite, which then reacts with the available pozzolanic oxides. High values of both the SO_3/K_2O ratio and high value of free lime lead to a decrease in initial shrinkage or an increase in initial swelling [52]. Analysis of the test results after 90 days of measurement showed that the addition of RTPF had a slightly positive effect on the reduction of long-term autogenous deformations. Based on previous studies [19-23], we can conclude that the greatest contribution of RTPF to the reduction in autogenous shrinkage is observed in the first 24 h after mixing. The effect of RTPF on early-stage autogenous deformations can be explained by the fact that the modulus of elasticity of the fibres is higher than that of the cement composites at early ages; therefore, the presence of these fibres has a positive effect on the stress distribution and strain capacity, minimising the potential for cracking under the tensile stresses generated by shrinkage. In addition, the lower value of autogenous shrinkage in mixtures with RTPF can be explained by the additional amount of water available on the surface of the fibres, which may play a key role in the reduced self-drying of cement composites and thus in the reduction of autogenous shrinkage [19, 53]. Considering the above results from previous studies on the positive effect of the addition of RTPF on the reduction of autogenous deformations and the results obtained in this study on the addition of WBA significantly contributing to the reduction of long-term autogenous deformations, a promising synergistic combination is proposed for the reduction of autogenous deformations in cement composites.

Table 7. Relative autogenous shrinkage compared with the reference mixtures

Autogenous shrinkage			
Days \ Mixture	M2	M3	M4
3	+307 %	+615.0 %	-708.0 %
7	-36.3 %	+140.6 %	-65.4 %
90	+6.4 %	+56.7 %	+62.2 %

3.5. Pore structure

The pore distribution was measured at 365 days using the MIP method, and both the cumulative and differential pore size distributions are shown in Figure 8.

The differential pore size distribution (Figure 8a) of the Mi-A samples showed that the M3-A sample was clearly prominent, where a higher proportion of pores above 0.1 μm occurred, which was not observed in the other samples. This was also observed in the M3-S samples. The differential pore size distribution was wider in the Mi-S samples than in the Mi-A samples. This effect was also observed in the cumulative pore size distribution (Figure 8), where samples cured at a RH of 60 ± 10 % and temperature of 21 ± 2 °C (Mi-S) were much coarser than those cured at an RH of 95 % and temperature of 20 ± 2 °C (Mi-A), which could be explained by suppressed hydration owing to the lack of water at 60 % RH [54]. The influence of RTPF and WBA addition on the pore structure was visible in the differential pore size distribution of Mi-S samples: with fibre addition (M2-S), the pore fraction less than 0.1 μm was higher, whereas the opposite was observed with WBA addition (M3-S).

Based on the MIP measurements, several pore size characteristics, such as the critical pore entry radius, median pore diameter, average pore diameter, and porosity, were analysed (Table 8). The critical radius is the inflection point on the curve of intruded volume vs. pore size, i.e. the pore radius corresponding to the peak value in the dV/dD curve [41], the median pore diameter (volume or area) as the median value is defined as the value at which half of the population resides above this point, and the average pore diameter or mean pore diameter is determined by the ratio between the total pore volume and pore surface area [55]. The results for the porosity of different sample curing times are shown in Figure 9, indicating significantly higher values for the Mi-S samples. The individual values of the critical pore entry radius for Mi-A were lower than those for Mi-S regardless of the curing conditions, except for the M2 specimens. All median and average pore diameters were lower for the Mi-A specimens.

The addition of WBA affected the microstructure of the cement composites. Reference [16] investigated the influence of WBA as a cement replacement on the pore structure of mortars

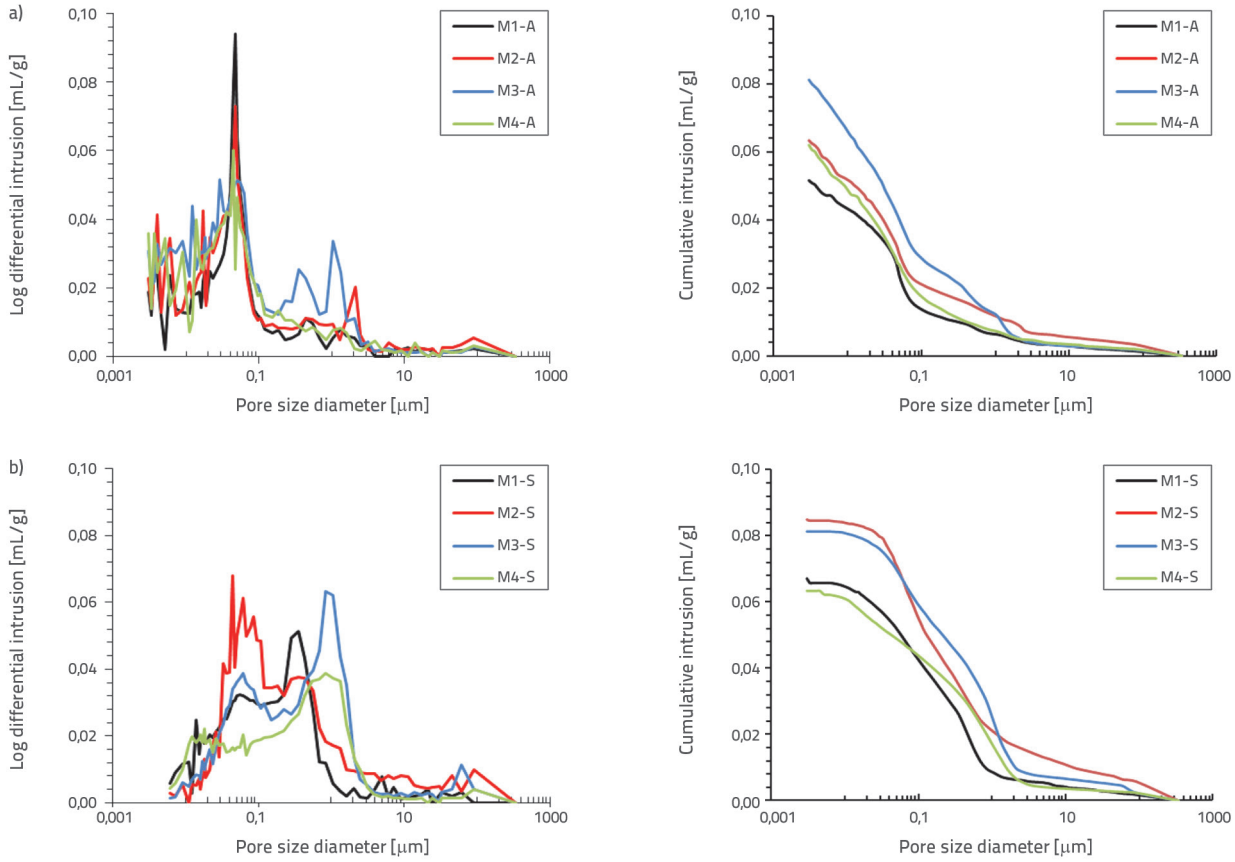

Figure 8. Differential pore size distribution (left) and cumulative pore size distribution (right) of: a) mortars samples cured at an RH of 95% and a temperature of 20 ± 2 °C and b) mortars samples cured at an RH of 60 ± 10% and temperature of 21 ± 2 °C

Table 8. Characterization of pore sized measured using MIP

Sample mark [μm]	Critical pore entry radius [μm]	Median pore diameter (volume) [μm]	Median pore diameter (area) [μm]	Average pore diameter [μm]	Porosity [%]
M1-A	0.0474	0.0475	0.0066	0.0196	11.3361
M2-A	0.0474	0.0473	0.0061	0.0186	13.4669
M3-A	0.0290	0.0489	0.0066	0.0190	16.7449
M4-A	0.0447	0.0397	0.0056	0.0164	13.3432
M1-S	0.4332	0.1994	0.0136	0.0491	14.5890
M2-S	0.0447	0.2118	0.0384	0.0853	17.4389
M3-S	0.8359	0.4559	0.0360	0.1051	17.0786
M4-S	0.8315	0.3737	0.0137	0.0545	14.0046

and observed a change in the pore structure: after 28 days, the samples with WBA exhibited an increase in total porosity compared with the reference mixture (1.6 % to 9.0 % for 10 %, and 5.3 % to 9.4 % for 20 % WBA as a cement replacement). Similar results were observed between M1-A and M3-A or M1-S and M3-S: for 15 % cement replacement by WBA, porosity increased by 47.7 % for M3-A and 17.1 % for M3-S.

Based on [56], to gain better insight into the pore size distribution as a function of curing conditions the authors in [55] divided the measured pore distribution into four size ranges: gel micropores (< 4.5 nm), meso-pores (4.5 to 50 nm), middle capillary pores (50–100 nm), and large capillary pores (> 100 nm). This method was used in this study and is shown in Figure 10. The pore proportions, listed by diameter, were obtained

from the proportion of mercury volume in the pore size interval to the total mercury volume within the specimen. The curing conditions had a significant effect on pore refinement: the proportion of gel and mesopores was higher for Mi-A specimens (54.6 % for M1-A, 53.1 % for M2-A, 50.8 % for M3-A, and 56.9 % for M4-A) compared with those cured at 60 % RH (22.8 % for M1-S, 16.5 % for M2-S, 14.4 %. % for M3-S and 22.9 % for M4-S). The change in microstructure was clearly observed in the change in mesopores (4.5 to 50 nm) in the Mi-A samples: with WBA addition, the mesopores decreased by 5 %, in the samples with RTPF by 3.6 %, whereas for M4, when WBA and RTPF were added, mesopores increased by 3.7 % compared with the control mixture. In the Mi-S samples, microstructural changes were visible in the form of a decrease in the middle capillary pores (50 to 100 nm) and an increase in the large capillary pores (> 100 nm) in M2-S, M3-S, and M4-S.

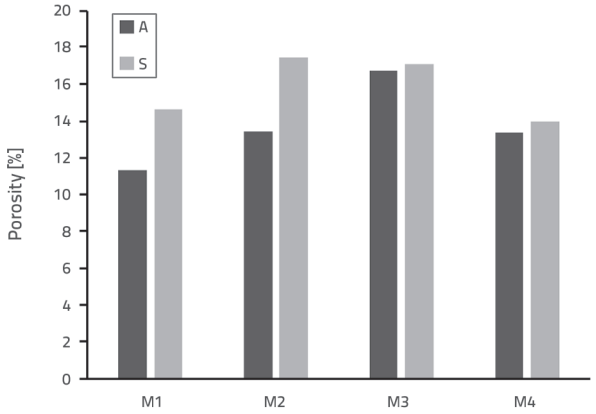

Figure 9. Porosity of blended cement mortars at different curing conditions by MIP measurement (S - mortars samples cured at an RH of 60 ± 10 % and temperature of 21 ± 2 °C and A - mortars cured at an RH of 95 % and a temperature of 20 ± 2 °C)

The pore structure, which includes the porosity of cement composites, pore size distribution, and pore morphology, plays an important role in the autogenous shrinkage behaviour of cement composites. The stresses caused by shrinkage lead to different water saturations in pores of different sizes, and the interconnectedness of these pores directly affects the migration of moisture from saturated to unsaturated pores, which ultimately affects autogenous shrinkage [57]. We observed that the use of RTPF and WBA had an effect on the pore structure of the mortars (Figure 10), and thus on the results of autogenous shrinkage (Figure 7). The autogenous shrinkage tended to decrease with the use of WBA and RTPF. Reference [58] claimed that the volumetric percentage of 5–50 nm pores is one of the main factors affecting autogenous shrinkage; the larger the volumetric percentage, the higher the autogenous shrinkage. These conclusions can be applied to this study: with the addition of WBA and RTPF (M2 and M3), the mesopores were smaller after 365 days, which was reflected in lower values of autogenous shrinkage compared with the reference mixture (M1). The synergic action of WBA and RTPF addition for M4 was not visible in pore structure; the volume percentage of mesopores was higher (3.7 %) than of reference, despite the reduced values of autogenous shrinkage mixture.

4. Conclusions

The main objectives of this study were to determine the synergistic effect and influence of fly wood biomass ash (WBA) and recycled tire polymer fibres (RTPF) on the long-term autogenous shrinkage and drying shrinkage of mortars and to determine the pore structure of mortar samples with fly WBA and RTPF. Tests were conducted on mortars in which the cement was replaced with 15 % WBA per cement mass, and 2 kg/m^3 of RTPF was added to some mixtures.

The greatest contribution to the reduction in drying shrinkage after 365 days was observed in the specimens with 15 % WBA as cement replacement, i.e. the reduction in shrinkage was 14 %, which was almost equal to the percentage of cement replacement by WBA. The addition of 2 kg/m^3 RTPF resulted in a slight reduction in drying shrinkage. The results of this study indicated that the addition of WBA and RTPF had no synergistic effect on the drying shrinkage of mortar, whereas this was not the case for long-term autogenous shrinkage. The greatest reduction in autogenous shrinkage was achieved by the addition of WBA and RTPF; autogenous shrinkage was reduced by 62 % after 90 days compared with the reference mixture. The results showed that the addition of WBA to mortars significantly contributes to long-term autogenous shrinkage, whereas this was not the case with the addition of RTPF, which had a minimal effect. In addition, the use of RTPF and WBA affects the pore structure of the mortar, and thus the autogenous shrinkage results. With the addition of RTPF (M2) and WBA (M3), the mesopores were smaller after 365 days,

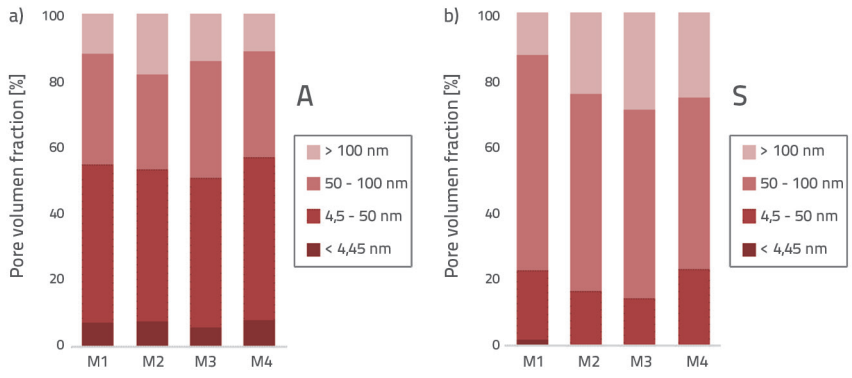

Figure 10. Pore volume distribution measured using MIP with pore classification from [42]: a) mortar samples treated at a relative humidity of more than 99.9 % and a temperature of 20 ± 2 °C; b) samples treated at a relative humidity of 60 ± 10 % and a temperature of 21 ± 2 °C

which was reflected in the lower values of autogenous shrinkage compared with the reference mixture, whereas the synergistic effect of WBA and RTPF addition (M4) on the volume fraction of the mesopores was not visible.

The results of this study are encouraging regarding the synergistic effect of using WBA and RTPF to reduce autogenous shrinkage. Nevertheless, future studies should investigate the optimal amount of WBA and RTPF for the greatest reduction in autogenous shrinkage while maintaining satisfactory fresh and mechanical properties and clarify the mechanism of action of WBA and RTPF on autogenous and drying shrinkage.

Acknowledgement

This research was performed as a part of the research project KK.01.2.1.01.0049 *Development of innovative construction products using bio-ash*, which was funded by the European Regional Development Fund.

REFERENCES

[1] Bjegović, D., Štirmer N.: Teorija i tehnologija betona, Sveučilište u Zagrebu Građevinski fakultet, Zagreb, 2015.

[2] Šahinagić-Isović, M., Markovski, G., Ćećez, M.: Deformations of concrete shrinkage - causes and types. Građevinar, 64 (2012) 9, 727-734, https://doi.org/10.14256/JCE.719.2012

[3] Holt, E.E.: Early Age Autogenous Shrinkage of Concrete, Espoo 2001, Technical Research Centre of Finland, VTT Publications 446, 2001, http://www.vtt.fi/inf/pdf/publications/2001/P446.pdf

[4] American Concrete Institute - ACI231-R, Report of Early-Age Cracking: Causes, Measurement, and Mitigation, 2010.

[5] Swamy, R.N., Stavrides, H.: Influence of Fiber Reinforcement on Restrained Shrinkage and Cracking. ACI Journal Proceedings, 76 (1979) 3, pp. 443-460, 1979, https://doi.org/10.14359/6954

[6] Saje, D., Bandelj, B., Šušteršič, J., Lopatič, J., Saje, F.: Autogenous and Drying Shrinkage of Fibre Reinforced High-Performance Concrete. Journal of Advanced Concrete Technology, 10 (2012) 2, pp. 59–73, https://doi.org/10.3151/jact.10.59

[7] American Concrete Institute - ACI 544.5R-10, Report on the Physical Properties and Durability of Fiber-Reinforced Concrete, 2010.

[8] Vassilev, S.V., Baxter, D., Andersen, L.K., Vassileva, C.G.: An overview of the composition and application of biomass ash. Part 1. Phase-mineral and chemical composition and classification, Fuel, 105 (2013), pp. 40–76, https://doi.org/10.1016/j.fuel.2012.09.041

[9] Milovanović, B., Štirmer, N., Carević, I., Baričević, A.: Wood biomass ash as a raw material in concrete industry, Građevinar, 71 (2019) 6, pp. 505–514, https://doi.org/10.14256/JCE.2546.2018

[10] Udoeyo, F.F., Inyang, H., Young, D.T., Oparadu, E.E.: Potential of wood waste ash as an additive in concrete, Journal of Materials in Civil Engineering, 18 (2006), pp. 605–611, https://doi.org/10.1061/(ASCE)0899-1561(2006) 18:4(605)

[11] Sigvardsen, N.M., Geiker, M.R., Ottosen, L.M.: Phase development and mechanical response of low-level cement replacements with wood ash and washed wood ash, Construction and Building Materials, 269 (2021) 1, https://doi.org/10.1016/j.conbuildmat.2020.121234

[12] Carević, I., Serdar, M., Štirmer, N., Ukrainczyk, N.: Preliminary screening of wood biomass ashes for partial resources replacements in cementitious materials, Journal of Cleaner Production, 229 (2019), pp.1045–64, https://doi.org/10.1016/j.jclepro.2019.04.321

[13] Cheah, C.B., Ramli, M.: The implementation of wood waste ash as a partial cement replacement material in the production of structural grade concrete and mortar: An overview, Resources, Conservation and Recycling, 55 (2011) 7, pp. 669–85, http://dx.doi.org/10.1016/j.resconrec.2011.02.002

[14] Chowdhury, S., Mishra, M., Suganya, O.: The incorporation of wood waste ash as a partial cement replacement material for making structural grade concrete: An overview, Ain Shams Engineering Journal, 6 (2015) 2, pp. 429–37, http://dx.doi.org/10.1016/j.asej.2014.11.005

[15] Yang, Z., Huddleston, J., Brown, H.: Effects of Wood Ash on Properties of Concrete and Flowable Fill, Journal of Materials Science and Chemical Engineering, 4 (2016), pp.101–114, 10.4236/msce.2016.47013

[16] Medina, J.M., Sáez del Bosque, I.F., Frías, M., Sánchez de Rojas, M.I., Medina, C.: Durability of new blended cements addition with recycled biomass bottom ASH from electric power plants, Construction and Building Material, 225 (2019), pp. 429–440, doi.org/10.1016/j.conbuildmat.2019.07.176

[17] Rosales, J., Cabrera, M., Beltrán, M.G., López, M., Agrela, F.: Effects of treatments on biomass bottom ash applied to the manufacture of cement mortars, Journal of Cleaner Production, 154 (2017), pp. 424–435, doi.org/10.1016/j.jclepro.2017.04.024

[18] Ukrainczyk, N., Vrbos, N., Koenders, E.A.B.: Reuse of Woody Biomass Ash Waste in Cementitious Materials, Chemical and Biochemical Engineering Quarterly, 30 (2016) 2, https://doi.org/10.15255/CABEQ.2015.2231

[19] Baričević, A., Jelčić Rukavina, M., Pezer, M., Štirmer, N.: Influence of recycled tire polymer fibers on concrete properties, Cement and Concrete Composites, 91 (2018), pp. 29–41, https://doi.org/10.1016/j.cemconcomp.2018.04.009

[20] Grubor, M., Štirmer, N., Jelčić Rukavina, M., Baričević, A.: Effect of recycled tire polymer fibers on autogenous deformation of self-compacting concrete, RILEM Technical Letter, 5 (2020), pp. 33–40, https://doi.org/10.21809/rilemtechlett.2020.115

[21] Baričević, A., Pezer, M., Jelčić Rukavina, M., Serdar, M., Štirmer, N.: Effect of polymer fibers recycled from waste tires on properties of wet-sprayed concrete, Construction and Building Materials, 176 (2018), pp.135–144. https://doi.org/10.1016/j.conbuildmat.2018.04.229

[22] Serdar, M., Baričević, A., Jelčić Rukavina, M., Pezer, M., Bjegović, D., Štirmer, N.: Shrinkage Behaviour of Fibre Reinforced Concrete with Recycled Tyre Polymer Fibres. International Journal of Polymer Science, 145918-1-145918-9 (2015). https://doi.org/10.1155/2015/145918

[23] Grubor, M.: Volume Deformations of Cement Composites with Recycled Tyre Polymer Fibers, PhD thesis, University of Zagreb, Faculty of Civil Engineering, Zagreb, 2020.

[24] Onuaguluchi, O., Banthia, N.: Durability performance of polymeric scrap tire fibers and its reinforced cement mortar, Mater. Struct. Constr. 50 (2017), https://doi.org/10.1617/s11527-017-1025-7.

[25] Figueiredo, F.P., Huang, S.S., Angelakopoulos, H., Pilakoutas, K., Burgess, I.: Effects of Recycled Steel and Polymer Fibres on Explosive Fire Spalling of Concrete, Fire Technol, 2019, https://doi.org/10.1007/s10694-019-00817-9.

[26] Figueiredo, F.P., Huang, S.S., Angelakopoulos, H., Pilakoutas, K., Burgess, I.: Fire protection of concrete tunnel linings with waste tyre fibres, Procedia Eng., 210 (2017), pp. 472–478, https://doi.org/10.1016/j.proeng.2017.11.103.

[27] Jelčić Rukavina, M., Baričevic, A., Serdar, M., Grubor, M.: Study on the post-fire properties of concrete with recycled tyre polymer fibres, Cement and Concrete Composites, 123 (2021) 104184, https://doi.org/10.1016/j.cemconcomp.2021.104184.

[28] Chen, M., Zhong, H., Zhang, M.: Flexural fatigue behaviour of recycled tyre polymer fibre reinforced concrete, Cement Concr. Compos., 105 (2020). https://doi.org/10.1016/j.cemconcomp.2019.103441

[29] Chen, G.M., Lin, C.J., Yang, H., He, Y.H., Zhang, H.Z., Chen, J.F.: Fracture behaviour of steel fibre reinforced recycled aggregate concrete after exposure to elevated temperatures, Construct. Build. Mater., 128 (2016) 272–286, https://doi.org/10.1016/j.conbuildmat.2016.10.072.

[30] The European Committee for Standardization: Methods of testing cement - Part 1: Determination of strength (EN 196-1:2016), 2016

[31] Gleize, P.J.P., Cyr, M., Escadeillas, G.: Effects of metakaolin on autogenous shrinkage of cement pastes, Cement and Concrete Composites, 29 (2007) 2, pp. 80–87, doi:10.1016/j.cemconcomp.2006.09.005

[32] The European Committee for Standardization: Fly ash for concrete - Part 1: Definition, specification and conformity criteria (EN 450-1:2013), 2013.

[33] Shah Kalpit, V., Cieplik, M.K., Betrand, C.I., van de Kamp, W.L., Vuthaluru, H.B.: Correlating the effects of ash elements and their association in the fuel matrix with the ash release during pulverized fuel combustion, Fuel Process and Technologies, 91 (2010) 5, pp. 531–545, http://dx.doi.org/10.1016/j.fuproc.2009.12.016

[34] Carević, I., Baričević, A., Štirmer, N., Bajto Šantek, J.: Correlation between physical and chemical properties of wood biomass ash and cement composites performances, Construction and Building Materials, 256 (2020), 10.1016/j.conbuildmat.2020.119450

[35] Berra, M., Mangialardi, T., Paolini, A.E.: Reuse of woody biomass fly ash in cement-based materials, Construction and Building Materials, 76 (2015), pp. 286–296, doi:10.1016/j.conbuildmat.2014.11.052.

[36] Kostanić Jurić, K., Carević, I., Serdar, M., Štirmer N.: Feasibility of using pozzolanicity tests to assess reactivity of wood biomass fly ashes, Građevinar, 72 (2020) 12, pp.1145–53, doi:https://doi.org/10.14256/JCE.2950.2020

[37] Carević, I., Štirmer, N., Serdar, M., Ukrainczyk, N.: Effect of wood biomass ash storage on the properties of cement composites, Materials (Basel), 14 (2021) 7, doi:10.3390/ma14071632

[38] Korat, L.: Characterization of the cement composites with mineral additives, Thesis, Ljubljana, 2015.

[39] Holmberg, S.L., Claesson, T.: Mineralogy of granulated wood ash from a heating plant in Kalmar, Sweden, Environmental Geology, 40 (2001), pp. 820–828, https://doi.org/10.1007/s002540100261

[40] Ukrainczyk, N., Koenders, E.A.B., Štirmer, N.: Transformation of wood ash waste into construction materials, Proceedings of the 1st International Conference on Construction Materials for Sustainable Future, pp. 101-108, 2017.

[41] Scrivener, K., Snellings, R., Lothenbach, B.: A Practical Guide to Microstructural Analysis of Cementitious Materials, 1st Edition, CRC Press, 2017.

[42] Sigvardsen, N.M., Kirkelund, G.M., Jensen, P.E., Geiker, M.R., Ottosen, L.M.: Impact of production parameters on physiochemical characteristics of wood ash for possible utilisation in cement-based materials, Resources, Conservation and Recycling, 145 (2019), pp. 230–40, https://doi.org/10.1016/j.resconrec.2019.02.034

[43] Cheah, C.B., Ramli, M.: Mechanical strength, durability and drying shrinkage of structural mortar containing HCWA as partial replacement of cement, Construction and Building Materials, 30 (2012), pp. 320–332, doi:10.1016/j.conbuildmat.2011.12.009

[44] Velay-Lizancos, M., Azenha, M., Martínez-Lage, I., Vázquez-Burgo, P.: Addition of biomass ash in concrete: Effects on E-Modulus, electrical conductivity at early ages and their correlation, Construction and Building Materials, 157 (2017), pp. 1126–1132. doi:: https://doi.org/10.1016/j.conbuildmat.2017.09.179

[45] Rajamma, R., Ball, R.J., Tarelho, L.A.C., Allen, G.C., Labrincha J.A., Ferreira V.M.: Characterisation and use of biomass fly ash in cement-based materials, Journal of Hazardous Materials, 172 (2009) 2–3, pp. 1049–1160, doi:10.1016/j.jhazmat.2009.07.109

[46] Naik, T.R., Kraus, R.N., Kumar, R.: Wood ash: A New Source of Pozzolanic Material, Vol. 435, Report No. CBU-2001-10. 2001, https://www4.uwm.edu/cbu/Papers/2001 CBU Reports/CBU 2001-11.pdf, 08.09.2018.

[47] Wang, S., Miller, A., Liamazos, E., Fonseca, F., Baxter, L.: Biomass fly ash in concrete: Mixture proportioning and mechanical properties, Fuel, 87 (2008) 3, pp. 365–371, doi:10.1016/j.jclepro.2020.123996

[48] Chen, M., Zhong, H., Chen, L., Zhang, Y., Zhang, M.: Engineering properties and sustainability assessment of recycled fibre reinforced rubberised cementitious composite, Journal of Cleaner Production, 278 (2021), pp. 123996, doi:10.1016/j.jclepro.2020.123996

[49] Bentz, D.P., Jensen, O.M.: Mitigation strategies for autogenous shrinkage cracking, Cement and Concrete Composites, 26 (2004), pp. 677–85, doi:10.1016/S0958-9465(03)00045-3

[50] Zhang, Y., Teramoto, A., Ohkubo, T.: Effect of addition rate of expansive additive on autogenous shrinkage and delayed expansion of ultra-high strength mortar, Journal of Advance Concrete Technology, 16 (2018), pp. 250–261, doi:10.3151/jact.16.250

[51] Nocuń-Wczelik, W., Bochenek, A., Nocun, W.: Calorimetry and other methods in the studies of expansive cement hydrating mixtures, Journal of Thermal Analysis and Calorimetry, 109 (2012) 2, pp. 529–535, doi:10.1007/s10973-012-2379-2

[52] Barcelo, L., Moranville, M., Clavaud, B.: Autogenous shrinkage of concrete: a balance between autogenous swelling and self-desiccation, Cement and Concrete Research, (2005), pp. 177–183, doi:10.1016/j.cemconres.2004.05.050

[53] Bentz, D.P.: A review of early-age properties of cement-based materials, Cement and Concrete Research, 38 (2008) 2, pp. 196–204, https://doi.org/10.1016/j.cemconres.2007.09.005

[54] Kanna, V., Olson, R.A., Jennings, H.M.: Effect of shrinkage and moisture content on the physical characteristics of blended cement mortars, Cement and Concrete Research, 28 (1998) 10, pp. 1467–1477. http://journal.unair.ac.id/download-fullpapers-ln522cc87c61full.pdf

[55] Zeng, Q., Li, K., Fen-Chong, T., Dangla, P.: Pore structure characterization of cement pastes blended with high-volume fly-ash, Cement and Concrete Research, 42 (2012) 1, pp. 194–204. http://dx.doi.org/10.1016/j.cemconres.2011.09.012

[56] Mehta, P.K., Monteiro, P.J.M.: Concrete, Microstructure, Properties and Materials, Third Edit. McGraw-Hill, 2006.

[57] Wu, L., Farzadnia, N., Shi, C., Zhang, Z., Wang H., Autogenous shrinkage of high performance concrete: A review, Constr Build Mater, 149 (2017), pp. 62–75.

[58] Li, Y., Bao, J., Guo, Y.: The relationship between autogenous shrinkage and pore structure of cement paste with mineral admixtures, Construction and Building Materials, 24 (2010) 10, pp. 1855–1860. http://dx.doi.org/10.1016/j.conbuildmat.2010.04.018